Application of Fe-Ni-W Plated Film Electrode to Zinc-Air Battery

Sachio Yoshihara*, Hikari Ohtake, Jiu Sasaki

Graduate School of Engineering, Utsunomiya University, Utsunomiya, Japan
Email: *sachioy@cc.utsunomiya-u.ac.jp

Abstract

This study was aimed at the preparation of an electrode for Zinc–air battery, which had excellent catalytic activity by use of electroplating of alloys made of abundant metal, such as Fe and Ni. The oxygen overvoltage of the Fe-Ni-W alloy plated electrode was the smallest through the measurement. The elemental composition and the enlargement of the surface area were confirmed by SEM and EDX analysis. Involvement of Fe and W of Fe-Ni-W alloy plated electrode will be one factor for its high catalytic activity. Thus plated Fe-Ni-W alloy electrodes were compared with other Fe alloy plated electrodes considering to their cathode performance as Zinc-air battery. The catalytic activity of Fe-Ni-W plated electrode showed the best performance comparing to Fe-Ni alloy plated electrodes as cathode for Zinc-air battery. Also comparing to the platinum electrode which had been widely used as cathode in the field of Zinc-air battery, the Fe-based alloy plated electrode showed better performance as the electrodes considering to its oxygen evolution reaction.

Keywords

Fe-Ni-W, Alloy, Electroplating, Zinc-Air Battery, Oxygen Evolution Reaction (OER)

1. Introduction

World energy consumption continues to increase along with economic growth, continuing to increase at an annual average of 2.6% from 1600 GJ in 1965, reaching 5300 GJ in 2013. The main energy source responsible for this huge energy consumption will be fossil fuel. More than 80% of the current world energy demand is covered by natural gas, coal and oil. Disadvantages of the society consuming such a large amount of fossil fuel have emerged as global warming and environmental pollution problems. In order to solve this problem,

conversion from fossil fuels to decarbonization and renewable energy, which is a low environmental load, should be a global issue [1] [2] [3]. For utilizing the renewable energy, energy storage system will be needed. Supposing electric energy as the second energy source, electric energy storage system will be indispensable.

Up to now, Li-ion batteries have been the most successful electric energy storage solution and widely used in portable electronics and electric vehicles (EVs). Unfortunately, their limitations of high cost, insufficient energy density, and poor safety have disturbed the large scale applications of Li-ion batteries in the automobile industry, especially for the extended range EVs. In this point, many post-lithium-ion technologies including Na-S and metal-air batteries have been investigated. Recently, metal-air batteries have become a promising power source, based on the nature of high theoretical energy density and free-oxygen fuel from the atmosphere. Among various metal-air batteries, alkaline metal-air batteries, especially lithium-oxygen, have been intensively investigated due to their high specific energy density up to 5200 $W \cdot h \cdot kg^{-1}$. However, the recharge ability, safety and cost issues make them hard to be commercialized. Because of these currently unconquerable limitations, rechargeable zinc-air batteries have attracted significant attention as an alternative in the past few years. As one of the most abundant elements in the earth's crust, zinc has been the chosen electrode material for several types of primary batteries ever since the past battery, *e.g.* Zinc-carbon battery. Primary zinc-air batteries were introduced to the science community in the late 19th century, and their commercial products started to enter the market in the 1930s. Among all metal-air systems, zinc-air batteries are the most practically variable choice. They possess some desirable features such as a high theoretical energy density, low cost, great safety and environmental friendliness. The theoretical energy density of zinc-air is 1086 $W \cdot h \cdot kg^{-1}$, about 5 times higher than that of Li-ion; its operational cost is estimated to be less than that of Li-ion. The primary zinc-air battery is a mature technology that has already been successfully applied to the fields of hearing, *etc.* Their recharge ability is realized by developing new bifunctional air cathodes and bifunctional oxygen electrocatalysts that can facilitate both the oxygen reduction reaction (ORR) during discharge and the oxygen evolution reaction (OER) during charge. Especially on bifunctional electrocatalysts for the air cathode, a comprehensive account of the current development status, challenges and possible solutions is highly necessary. Here in this paper, we focus on the fabrications of the air cathode of the electrically rechargeable and/or zinc-air batteries in alkaline electrolytes. We will propose newly developed air cathode of the rechargeable zinc-air battery, with higher bifunctional performance.

2. Experimental

2.1. Method for Manufacturing Alloy Plated Electrode

Stainless steel (SUS 430) which is relatively inexpensive and has good corrosion resistance was selected as a substrate to be subjected to electroplating treatment.

It is general to apply nickel strike plating as a pretreatment to a plating material which is prone to generate an oxide film on the surface like stainless steel. **Table 1** shows the plating conditions for nickel strike. The stainless steel substrate was degreased with acetone, followed with and distilled water, and then immersed in concentrated hydrochloric acid for 2 minutes to remove the oxide film. After washing above specimen with distilled water, Nickel strike plating was performed under constant current electrolytic method using an electrochemical measurement system (HA 305 Hokuto Denko Co., Ltd.) [4]. After that, masking was done so that the surface active area was 4 cm^2 by use of masking tape (N-300 Nitto Denko Co., Ltd.).

Table 2, **Table 3** show the bath composition and plating conditions for Fe-Ni alloy plating, Fe-Ni-W alloy plating, respectively. For the counter electrode, Ni electrode having sufficiently large surface area with respect to the cathode was used.

2.2. Elemental, Crystal Structure Analysis and Surface Observation Method of Coated Surface

The surface of the electrode was observed with a field emission scanning electron

Table 1. Bath composition and plating conditions for nickel-strike plating based on wood baths.

Bath composition	mol/dm³
NiCl$_2$	1.010 mol/dm^3
HCl	1.850 mol/dm^3
Plating Conditions	
Current density	100 mA/dm^2
Plating period	2 min
Bath temperature	22˚C - 25˚C
Counter electrode	Ni plate

Table 2. Bath composition and plating condition of Fe-Ni alloy plating.

Bath composition	mol/dm³
FeSO$_4$·7H$_2$O	0.050
NiSO$_4$·6H$_2$O	0.099
H$_3$BO$_3$	0.243
C$_2$H$_8$O$_7$	0.026
Plating Conditions	
Current density	25 mA/dm^2
Plating period	20 min
Bath temperature	40˚C
pH	2.50
Counter electrode	Ni plate

Table 3. Bath composition and plating conditions for Fe-Ni-W alloy plating.

Bath composition	mol/dm³
$FeSO_4 \cdot 7H_2O$	0.04
$NiSO_4 \cdot 6H_2O$	0.08
$Na_2WO_4 \cdot 2H_2O$	0.12
H_3BO_3	0.16
$C_2H_8O_7$	0.02
$C_6H_5Na_3O_7 \cdot 2H_2O$	0.19
Plating Conditions	
Current density	50 mA/dm²
Plating period	30 min
Bath temperature	75°C
pH	7.3
Counter electrode	Ni plate

microscope (FE-SEM, Hitachi Co. Ltd., S-4500). The surface condition was observed at an accelerating voltage of 15 kV.

For the purpose of qualitative and quantitative analysis of the surface, the evaluation by an energy dispersive X-ray analyzer (Horiba Co. Ltd., EMAX-5770) was carried out under the conditions of an acceleration voltage of 20 kV and a probe current of −0.2 nA.

Crystal structure analysis of samples by XRD (X-ray diffraction) were carried out by use of the horizontal-type multi-purpose X-ray diffractometer (Rigaku Co. Ltd., Ultima IV) under CuK_a as X-ray source, 2θ/deg 20° - 90° of scanning range, 4°/min of scanning speed.

2.3. Method and Conditions of Electrolysis Test

LSV (linear sweep voltammetry) was carried out to evaluate the activity of the oxygen-evolution reaction, or the oxygen reduction reaction by use of electrochemical measurement system (Hokuto Denko Co. Ltd., HZ-5000). The electrolytic solution was 0.1 mol/dm³ KOH (industrial flaky KOH 95.5%: Japan Soda Co. Ltd.) aqueous solution. Counter and reference electrode were Platinum mesh and SCE electrode, respectively. LSV measurement was carried out under room temperature (25°C), potential sweep rate of 10 mV/s.

Tafel plots, plots the logarithm of current density against electrode potential, were used for the analysis of oxygen evolution reaction mechanism. The exchange current density and Tafel slope could be obtained from the Tafel plots.

In the case of evaluation of oxygen reduction reaction, in advance O_2 gas was bubbled in the solution for 30 minutes before LSV measurement, blank LSV were carried out also in the solution after bubbling N_2 for 30 minutes.

Real oxygen reduction current were estimated by taking the difference between the current measured after O_2 bubbling and that measured after N_2 bubbling.

3. Results and Discussions

3.1. Surface Analysis of Fe-Ni and Fe-Ni-W Alloy Plated Film

The surface composition analysis of alloy plating films using EDX results were shown in **Table 4**. It was confirmed that each films were made of metals contained in each plating bath.

Figure 1 shows SEM images of Fe-Ni, Fe-Ni-W plated films. The surface of Fe-Ni was smooth, on the other hand that of Fe-Ni-W were consisted of a number of small grains.

XRD analysis of crystal structure was shown in **Figure 2**. According to the results of the Fe-Ni-W, broadband 45° peak suggested the amorphous-like structure. Obtained crystallite grain size by Scherrer equation were 2.93 nm, 12.3 nm for Fe-Ni-W, Fe-Ni plated films, respectively. The crystallite size of Fe-Ni-W was smaller than that of Fe-Ni.

3.2. Electrolytic Test

LSV measurements of oxygen evolution reaction were shown in **Figure 3**. LSV

Table 4. Elemental analysis of alloy plating films (wt%).

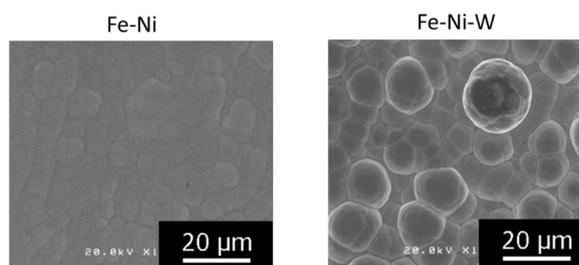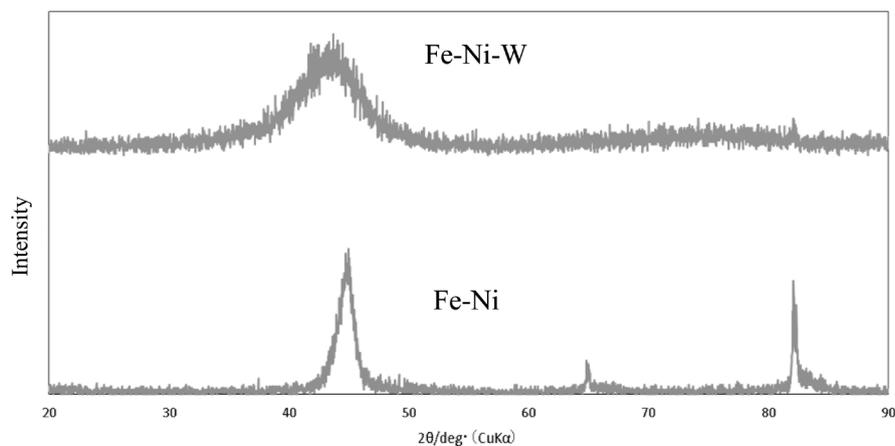|	Fe	Ni	W
Fe-Ni	70.0	30.0	-
Fe-Ni-W	28.0	27.6	44.4

Figure 1. SEM photopraphs.

Figure 2. XRD chart.

for Pt plate were also shown for comparison. Comparing current density at the same potential, Fe-Ni-W showed the largest current and Pt showed the lowest. Fe-Ni-W showed the highest activity for oxygen evolution reaction [5].

Tafel plot analysis results were shown in **Figure 4**. Tafel slope and exchange current density calculated from these Tafel plots were shown in **Table 5**. It was suggested that Fe-Ni-W showed relatively high activity for oxygen evolution reaction.

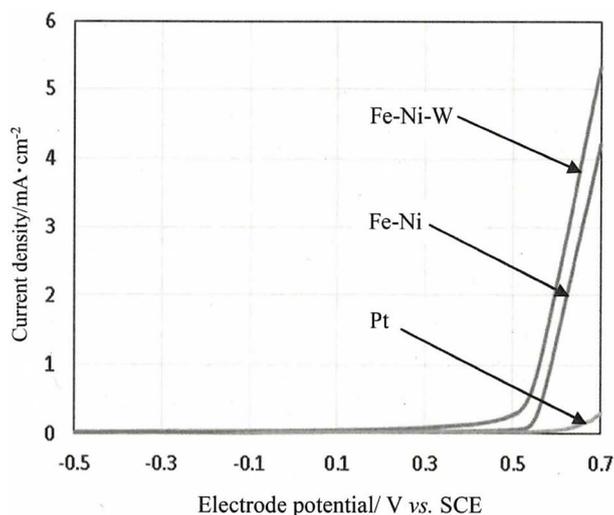The Tafel slope suggested the rate determining step (rds) for oxygen evolution
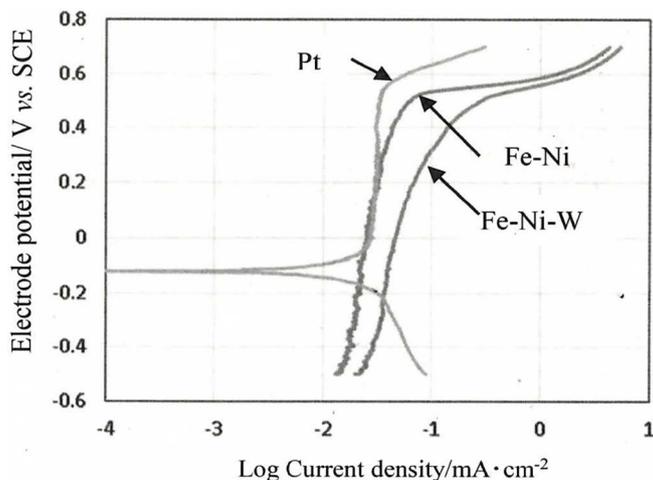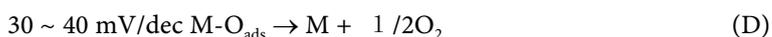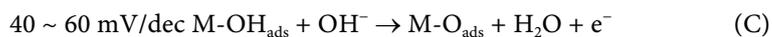

Figure 3. LSV for OER.

Figure 4. Tafel plots.

Table 5. Summarized Tafel data.

	Tafel slope [mV/dec]	Exchange current density[mA/cm²]
Fe-Ni-W	89.4	0.19
Fe-Ni	64.7	0.08
Pt	130.5	1.03×10^{-4}

reaction on each electrode. These could be classified into four groups. The Tafel slope value for each rds step were summarized as follows,

$$120 \text{ mV/dec} \quad M + OH^- \rightarrow M\text{-}OH_{ads}{}^* + e^- \tag{A}$$

$$60 \sim 120 \text{ mV/dec} \quad M\text{-}OH_{ads}{}^* \rightarrow M\text{-}OH_{ads} \tag{B}$$

$$40 \sim 60 \text{ mV/dec} \quad M\text{-}OH_{ads} + OH^- \rightarrow M\text{-}O_{ads} + H_2O + e^- \tag{C}$$

$$30 \sim 40 \text{ mV/dec} \quad M\text{-}O_{ads} \rightarrow M + \ 1/2O_2 \tag{D}$$
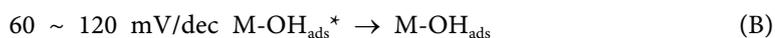
The rds step for OER on Fe-Ni, Fe-Ni-W electrode will be (B) process, on the other hand that on Pt will be (A) process. On platinum electrode OH^- adsorption activity for oxygen evolution reaction is inferior to that of Fe-Ni-W or Fe-Ni. On Fe-Ni-W or Fe-Ni electrode OH^- could adsorp easier to platinum. But it takes much time to form "stable" M-OH $_{ads}$ from "instable" M-OH$_{ads}{}^*$. In addition, visual observation confirmed that more oxygen bubbles on Pt electrode remained on the surface under operation comparing to that of Fe-Ni-W or Fe-Ni. Such easy release of evolved oxygen bubbles might be one reason for high activity for oxygen evolution reaction on Fe-Ni-W or Fe-Ni electrode. SEM observation suggested that Fe-Ni-W plated electrode had rough surface (increase of the surface area) comparing to that of Fe-Ni, it might be one reason for high activity for oxygen evolution reaction on Fe-Ni-W.

LSV for the oxygen reduction reaction were shown in **Figure 5**. LSV for Pt plate was also shown for comparison. Comparing the current density at the same potential, Pt showed the largest reduction current. Also, the onset potential for reduction current on the iron-plated electrode were less noble to that of Pt plate electrode. The interface between vapor and liquid and solid-phase is important for oxygen reduction reaction. This suggests that the reason of decreased activity of the iron-plated electrode will be due to poor affinity between Fe-alloy and O_2. As mentioned above it was confirmed that more oxygen bubbles on Pt electrode remained on the surface under oxygen evolution reaction. This suggests that the affinity between Pt and O_2 will be stronger comparing to that between Fe-alloy
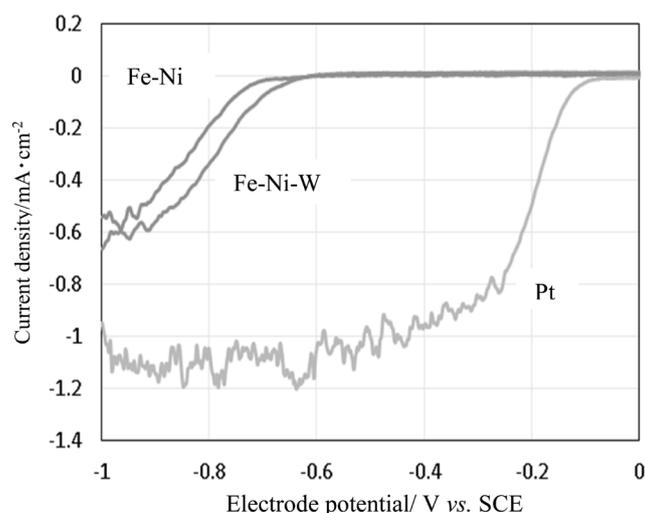

Figure 5. LSV for ORR.

and O$_2$. So such a well formed three-phase surface in the case of Pt electrode could reduce the dissolved oxygen in electrolyte. On the other hand quick release of O$_2$ on the Fe-alloy electrode induced large overpotential, small current density. Oxygen reduction reaction mechanism has not been cleared in detail, but oxygen-metal coupling strength will be due to the strength of covalent bonds of the 2 p orbital of oxygen and metal d-orbital. W (tungsten) having 5d orbital electron as well as Pt leads to dissociative adsorption of oxygen molecules so the activity of Fe-Ni-W was superior to that of Fe-Ni.

4. Conclusions

This study was aimed at the preparation of the air cathode for Zinc–air battery, which had excellent catalytic activity by use of electroplating of alloys made of abundant metal, such as Fe and Ni. Finally iron based alloy plated electrodes, especially Fe-Ni-W plated electrode were highly active for oxygen evolution reaction in compared to Pt from the results of the exchange current density obtained from LSV measurement, Tafel plots. The iron-based alloy coated electrode tends to be adsorbed by OH$^-$ species, successively release the evolved oxygen away from the surface, thus improves the oxygen evolution reaction activity. SEM, XRD observations revealed that Fe-Ni-W plated electrode, having increased surface area caused by the roughness of it, had a fine crystalline structure than that of the Fe-Ni. In the present study, considering to the oxygen reduction activity, comparing to Pt, iron-plated electrode showed a smaller current density and high overvoltage for oxygen reduction reaction. It will be attributed to poor forming of good critical gas/liquid/solid interface between oxygen reduction in aqueous solution. In addition, oxygen-metal coupling strength will be due to the strength of covalent bonds of the 2 p orbital of oxygen and metal d-orbital. W (tungsten) having 5d orbital electron as well as Pt leads to dissociative adsorption of oxygen molecules so the activity of Fe-Ni-W was superior to that of Fe-Ni.

Further study of the iron-plated electrode for oxygen reduction reaction will be needed for the practice use of such an electrode as the air cathode for metal-air batteries.

Conflicts of Interest

The authors declare no conflicts of interest regarding the publication of this paper.

References

[1] Denkikagaku, A. (2002) ECSJ Ed., Baifukan.

[2] NEDO Suiso Enerugii Hakusho (2015) NEDO Ed.

[3] Dresselhaus, M. and Thomas, I. (2001) *Nature*, **414**, 332.

[4] Mekkigijyutu, S. (2011) Kantogakuin Univ. Ed., Maruzen.

[5] Tong, Y., Yu, X. and Shi, G. (2017) *Phys. Chem. Chem. Phys.*, **19**, 4821-4826.